Proc. Int. Symposium on Neutron Optics and Related Research Facilities, Kumatori, 1996
J. Phys. Soc. Jpn. **65** (1996) Suppl. A pp. 203-206

Traversal Time through Magnetic Thin Film Using Larmor Precession

Masahiro HINO, Norio ACHIWA, *Seiji TASAKI, *Toru EBISAWA, *Tsunekazu AKIYOSHI and *Takeshi KAWAI

Department of Physics, Kyushu University, Fukuoka, Japan 812
**Research Reactor Institute, Kyoto University, Osaka, Japan 590-04*

(Received 18 March 1996; accepted 17 July 1996)

Authors have measured traversal times transmitted through magnetic thin films (iron or permalloy) with various thicknesses using Larmor precession of neutron spin as a clock. By inserting the magnetic film in one of the Larmor precession fields of a transverse neutron spin echo(NSE) instrument, the extra Larmor precessions were measured at various incident angles above the critical angle of total reflection. The magnetic induction in these magnetic thin films was measured with a SQUID magnetometer. A birefringence of neutron in the magnetic film produces different path lengths for ↑ and ↓ spin neutrons. Even in the vicinity of the critical angle, the Larmor precession was observed and the Larmor precessions were reproduced well by the simulation based on the one-dimensional Schrödinger equation. When we consider the classical image of Larmor precession, the observed traversal path length l corresponds well to a traversal path calculated from only the nuclear potential in the magnetic film above the critical angle.

KEYWORDS: Neutron spin echo(NSE), Larmor precession, birefringence of neutron

§1. Introduction

Though there have been some neutron experimental proposals to measure the traversal time of neutron across a magnetic thin film using Larmor precession as a clock [1], they have not been performed up to the present. This present paper is the first trial to measure the traversal time and was performed by using neutron spin echo(NSE) method [2].

A magnetic field exerts a torque on the neutron magnetic moment and the moment precesses about the direction of the field with Larmor frequency ω_L. The resulting equation of motion in a homogeneous magnetic field $\boldsymbol{B}$ is [3]

$$\frac{d\boldsymbol{S}}{dt} = -\gamma\boldsymbol{S}\times\boldsymbol{B} = \boldsymbol{S}\times\omega_L, \tag{1.1}$$

$$\omega_L = |\gamma|\boldsymbol{B}. \tag{1.2}$$

Thereby, if the field and the magnetic moment μ of the neutron have different directions, one observes a precession of μ about $\boldsymbol{B}$. In a homogeneous magnetic field, the Hamiltonian is

$$\hat{\mathcal{H}} = \hat{\mathcal{H}}_0 - \mu B, \tag{1.3}$$

$$\hat{\mu} = \frac{1}{2}\mu\hat{\sigma}, \hat{\sigma} = (\sigma_x, \sigma_y, \sigma_z), \tag{1.4}$$

$$\sigma_x = \begin{pmatrix} 0 & 1 \\ 1 & 0 \end{pmatrix}, \sigma_y = \begin{pmatrix} 0 & -i \\ i & 0 \end{pmatrix}, \sigma_z = \begin{pmatrix} 1 & 0 \\ 0 & -1 \end{pmatrix}. \tag{1.5}$$

where $\hat{\mathcal{H}}$ is the free particle term, $\hat{\mu}$ and μ the neutron magnetic moment operator and the magnitude of the magnetic moment respectively, and σ_x, σ_y, σ_z the Pauli matrices. The neutron spin is represented as superposition of wave functions between two Stern-Gerlach states $|\uparrow\rangle$ and $|\downarrow\rangle$ along direction z [4]. These states correspond to two Zeeman energies levels. The quasi-stationary wave function can be described as

$$|\psi(\boldsymbol{r},t)\rangle = e^{ik_0 r}\left[\exp\left(-\frac{i}{\hbar}|\mu B|t\right)|\uparrow\rangle + \exp\left(\frac{i}{\hbar}|\mu B|t\right)|\downarrow\rangle\right] \tag{1.6}$$

where $\begin{pmatrix} 1 \\ 0 \end{pmatrix}$ and $\begin{pmatrix} 0 \\ 1 \end{pmatrix}$ are the eigenstates of $|\uparrow\rangle$ and $|\downarrow\rangle$, respectively. From Eq. (1.6),

$$\begin{aligned}\langle S_x(t)\rangle &= \langle\psi(\boldsymbol{r},t)|\frac{\hbar}{2}\sigma_x|\psi(\boldsymbol{r},t)\rangle \\ &= \frac{\hbar}{2}\left(\exp\left(\frac{2i}{\hbar}|\mu B|t\right) + \exp\left(\frac{-2i}{\hbar}|\mu B|t\right)\right) \\ &= \hbar\cos\left(\frac{2|\mu B|t}{\hbar}\right) = \hbar\cos(\omega_L t)\end{aligned} \tag{1.7}$$

can be obtained. This behavior of the observable $\langle S_x \rangle$ is called the Larmor precession, and the Larmor frequency is $\omega_L = \dfrac{2|\mu B|}{\hbar}$. From $\delta = \omega_L t$, Eq.(1.6) is described as

$$\begin{aligned}|\psi(\boldsymbol{r},t)\rangle &= \begin{pmatrix} e^{ik_+ r} \\ e^{ik_- r} \end{pmatrix} = e^{ik_0 r}\begin{pmatrix} e^{-(i\omega_L t)/2} \\ e^{(i\omega_L t)/2} \end{pmatrix} \\ &= e^{ik_0 r}\begin{pmatrix} e^{-i\delta/2} \\ e^{i\delta/2} \end{pmatrix}.\end{aligned} \tag{1.8}$$

Therefore, the phase of the Larmor precession $\langle S_x \rangle$ corresponds to the time dependent change of phases of the wave functions of ↑ and ↓ spin neutrons.

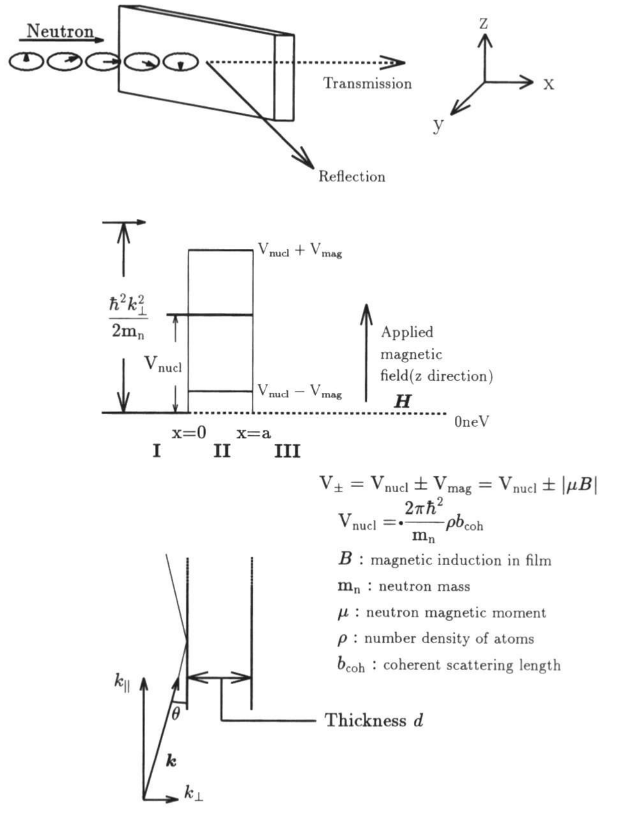

Fig.1. Schematic view of a Larmor precessing neutron entering into a magnetic film at an incident angle θ.

Here the problem of refraction and reflection of a neutron beam at a surface of a medium is considered as a one-dimensional Schrödinger equation [5]. Let us consider the condition shown in Fig.1 for various incident angles above the critical angle. From Eq.(1.8), the wave function of the incident beam for ideal Larmor precession is given by

$$|\psi\rangle = \frac{1}{\sqrt{2}}\begin{pmatrix} e^{-i\delta/2} \\ e^{i\delta/2} \end{pmatrix} e^{ikx}, \qquad (1.9)$$

where δ is equal to the Larmor phase for arbitrary neutron spin direction and this phase increases across the applied magnetic field $\boldsymbol{H}$.

In the transmission case, the Hamiltonian is diagonal using this spinor basis. Thus we can solve the one-dimensional Schrödinger equation for both $\hbar/2$ and $-\hbar/2$ spin case separately. Then the wave functions in the three regions are

Region I (x<0) :

$$\psi_{I(+)} = e^{ik_\perp(+)x} e^{-\frac{i\delta}{2}} + A_+ e^{-ik_\perp(+)x} \qquad (1.10)$$

$$\psi_{I(-)} = e^{ik_\perp(-)x} e^{\frac{i\delta}{2}} + A_- e^{-ik_\perp(-)x} \qquad (1.11)$$

$$k_{\perp(\pm)} = \frac{\sqrt{2m_n(E_\perp \mp |\mu H|)}}{\hbar}, E_\perp = \frac{(\hbar k_\perp)^2}{2m_n} \qquad (1.12)$$

Region II (0<x<a) :

$$\psi_{II(+)} = B_+ e^{iK_+ x} + C_+ e^{-iK_+ x} \qquad (1.13)$$

$$K_+ = \frac{\sqrt{2m_n(E_\perp - (V_{nucl} + |\mu B|))}}{\hbar} \qquad (1.14)$$

$$\psi_{II(-)} = B_- e^{iK_- x} + C_- e^{-iK_- x} \qquad (1.15)$$

$$K_- = \frac{\sqrt{2m_n(E_\perp - (V_{nucl} - |\mu B|))}}{\hbar} \qquad (1.16)$$

Region III (x>a) :

$$\psi_{III(+)} = D_+ e^{ik_{\perp(+)}x}, \qquad (1.17)$$

$$\psi_{III(-)} = D_- e^{ik_{\perp(-)}x}. \qquad (1.18)$$

The coefficients $D_\pm$ multiplying $e^{ik_\perp x}$ of the transmitted wave are obtained as [6]

$$D_+ = T_+^{1/2} e^{i\Delta\phi_+} e^{-ik_{\perp(+)}d} e^{-i\delta/2},$$
$$D_- = T_-^{1/2} e^{i\Delta\phi_-} e^{-ik_{\perp(-)}d} e^{i\delta/2}. \qquad (1.19)$$

Here $T_\pm$ are the transmission probabilities given by

$$T_+ = \left(1 + \frac{(k_{\perp(+)}^2 - K_+^2)^2}{4k_{\perp(+)}^2 K_+^2} \sin^2(K_+ d)\right)^{-1}$$

$$T_- = \left(1 + \frac{(k_{\perp(-)}^2 - K_-^2)^2}{4k_{\perp(-)}^2 K_-^2} \sin^2(K_- d)\right)^{-1} \qquad (1.20)$$

The phases increase across the barrier $\Delta\phi_\pm$ are determined by

$$\tan(\Delta\phi_+) = \frac{k_{\perp(+)}^2 + K_+^2}{2k_{\perp(+)} K_+^2} \sin^2(K_+ d),$$

$$\tan(\Delta\phi_-) = \frac{k_{\perp(-)}^2 + K_-^2}{2k_{\perp(-)} K_-^2} \sin^2(K_- d). \qquad (1.21)$$

The state of the spin of the transmitted neutrons is determined by

$$|\psi\rangle = (|D_+|^2 + |D_-|^2)^{-(1/2)} \begin{pmatrix} D_+ \\ D_- \end{pmatrix}. \qquad (1.22)$$

The expectation values of $\langle S_x \rangle$, $\langle S_y \rangle$ and $\langle S_z \rangle$ are given by

$$\langle S_x \rangle = \hbar\langle\psi|\frac{1}{2}\sigma_x|\psi\rangle = \frac{\hbar}{2}\frac{D_+ D_-^* + D_+^* D_-}{|D_+|^2 + |D_-|^2} \qquad (1.23)$$

$$\langle S_y \rangle = \hbar\langle\psi|\frac{1}{2}\sigma_y|\psi\rangle = \frac{\hbar}{2} i \frac{D_+ D_-^* - D_+^* D_-}{|D_+|^2 + |D_-|^2} \qquad (1.24)$$

$$\langle S_z \rangle = \hbar\langle\psi|\frac{1}{2}\sigma_z|\psi\rangle = \frac{\hbar}{2}\frac{|D_+|^2 - |D_-|^2}{|D_+|^2 + |D_-|^2} \qquad (1.25)$$

From Eq. (1.20), these expectation values can be rewritten as follows:

$$\langle S_x \rangle = \hbar\cos(\Delta\phi_+ - \Delta\phi_- - \delta)\frac{\sqrt{T_+ T_-}}{T_+ + T_-}, \qquad (1.26)$$

$$\langle S_y \rangle = -\hbar\sin(\Delta\phi_+ - \Delta\phi_- - \delta)\frac{\sqrt{T_+ T_-}}{T_+ + T_-}, \qquad (1.27)$$

$$\langle S_z \rangle = \frac{\hbar}{2}\frac{T_+ - T_-}{T_+ + T_-}. \qquad (1.28)$$

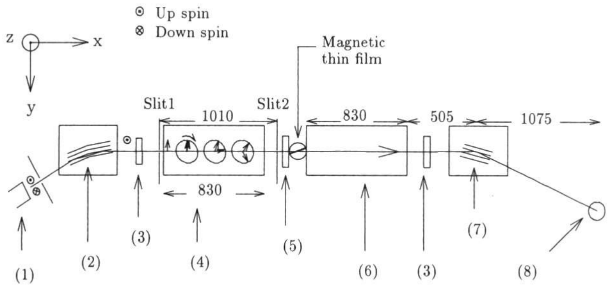

Fig. 2. The layout of neutron spin interference experiment using transverse NSE instrument. The size of both slit1 and slit2 are $0.5^{(y)} \times 10^{(z)}$ mm^2. The elements of the NSE instrument: (1) CN3 supermirror neutron guide tube, (2) Soller type Double reflection supermirror polarizer, (3) $\pi/2$ spin flipper coil, (4) First Larmor precession field, (5) π spin flipper coil, (6) Second Larmor precession field, (7) Soller type supermirror analyzer, (8) ^{3}He neutron detector.

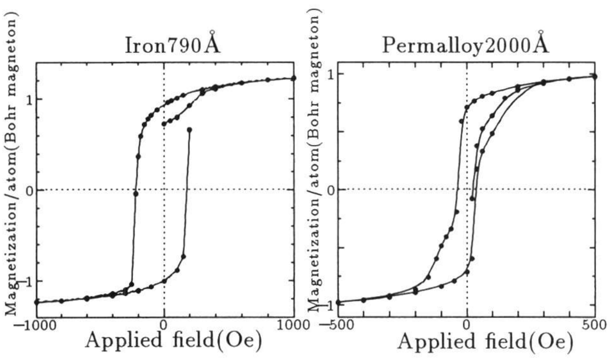

Fig.3. Magnetic induction in an iron film and a permalloy45 film with thickness of 790 and 2000 Å as a function of applied magnetic field measured by SQUID magnetometer. The closed circles are measured values and the line is calculated value by a spline function.

Eqs. (1.26) ~ (1.28) satisfy the requirement

$$\langle S_x \rangle^2 + \langle S_y \rangle^2 + \langle S_z \rangle^2 = \frac{1}{4}\hbar^2. \quad (1.29)$$

When the magnetic film is removed ($B = H$, $V_{nucl} = 0$) and $\delta = 0$, $\langle S_x \rangle$, $\langle S_y \rangle$ and $\langle S_z \rangle$ are

$$\langle S_x \rangle = \hbar \cos(\Delta\phi_+ - \Delta\phi_-), \quad (1.30)$$

$$\langle S_y \rangle = -\hbar \sin(\Delta\phi_+ - \Delta\phi_-), \quad (1.31)$$

$$\langle S_z \rangle = 0. \quad (1.31)$$

This expectation $\langle S_x \rangle$ corresponds to the Larmor precession of the neutron in a homogeneous magnetic field.

§.2 Experimental

Figure 2 shows the layout of this measurement using the transverse NSE instrument.[7),8)] The polarizer of double reflection type [9)] is an assembly of magnetic supermirrors of Soller slit type, and it provides a collimated, monochromatic, polarized beam with a negligible amount of $\lambda/2$ contamination. The magnetic supermirrors are made of $Fe_{50}Co_{50}$ -V multilayers with varying spacings from 70 to 90 Å. The distribution of wavelengths in the beam from the polarizer and slits system of the NSE instrument was measured by time-of-flight (TOF). The mean value of the wavelength distribution is 5.8 Å and the distribution is well fitted by a Gaussian function with standard deviation $\sigma_{\delta\lambda} = 0.287$ Å. The analyzer is an assembly of magnetic supermirrors of Soller slit type, and the magnetic supermirrors are made of $Fe_{50}Co_{50}$-V multilayers with widely varying spacings from 67.5 to 112.5 Å.

The experiments were carried out with changing incident angle of the magnetic film which was inserted in the transverse NSE instrument as shown in Fig. 2. The wavelength resolution was 5.8±0.67(FWHM) Å and the divergent angle was 0.990×10^{-3} rad. The incident angle was controlled by goniometer and the angle was calibrated by measuring the position of the direct and reflected beams by scanning a detector along the y direction.

The films were deposited on a silicon wafer of size $130\times65\times0.6$mm^3 in an applied magnetic field of 140Oe. The films can be saturated under lower magnetic field if the magnetic field is applied to the film during evaporation [10)]. A quartz crystal oscillator was used, and the thickness measured by the monitor was almost the same as that obtained by the neutron diffraction method, However, as the thickness is very important for this study, we reconfirmed the thickness by using a neutron reflectometer [11)] at JRR-3M reactor at JAERI. The magnetic induction in magnetic films were measured with a SQUID magnetometer at Kyushu University. The magnetic induction in magnetic films could also be measured by the shift of NSE signal. However it is important to estimate the degree of saturation of the film as a function of applied magnetic field.

Here the effect of the magnetic field during deposition was found in the residual magnetization as shown in Fig. 3. The saturated magnetization per atom for iron and permalloy45 films are 1.25 and 0.98 Bohr magneton with thicknesses of 790 and 2000Å, respectively, and they are smaller than the magnetization of bulk iron and permalloy45(2.2 and 1.5 Bohr magneton, respectively). The result also may be due to a reduction of the density of thin films and the error in the size.

The NSE signals transmitted through a magnetic thin film were measured at various incident angles. The incident angles give various potentials. At first, let us consider that ↑ and ↓ spin neutrons simply pass through a magnetic thin film, so that the incident angles are above the critical angle of both ↑ and ↓ spin neutrons. In the vicinity of the critical angle, birefringence of a neutron in the magnetic thin film produces different path lengths for ↑ and ↓ spin neutrons during Larmor precession as shown in Fig.4.

§.3. Results and Discussion

After transmission through the magnetic film, ↑ and ↓ spin neutrons have different phases in the spatial wave function. Fig. 5 shows the shifts of NSE signals (echo points) at various incident angles of an iron film with a thickness of 790 Å, and Fig. 6 shows those of a permalloy45 film with a thickness of 2000 Å. Here the nuclear and magnetic potentials of the iron film are assumed to be 209neV and 90.4neV, and those of the Permalloy 45 film are assumed to be 220neV and

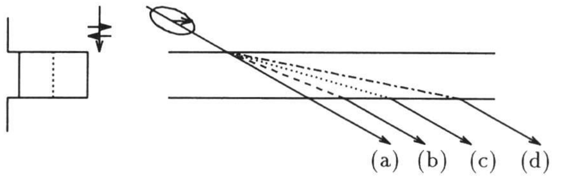

Fig.4. Schematic view of classical neutron paths due to refractions. (a) passing without refraction, (b) refraction path of ↓ spin, (c) refraction path due to only nuclear potential and (d) refraction path of ↑ spin neutrons.

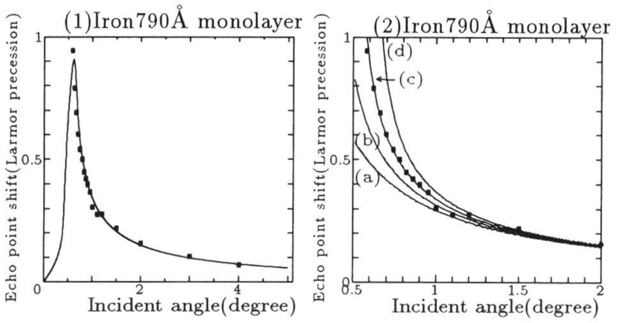

Fig. 5. The shift of NSE signals transmitted through magnetic iron thin film with thickness of 790 Å as a function of incident angle. The closed circles were measured and the solid line for (1) was calculated from matrix analysis of neutron spin rotation and of one-dimensional square potential for Schrödinger equation, and for (2) was calculated from the Larmor frequency ω_L and classical paths of neutron.

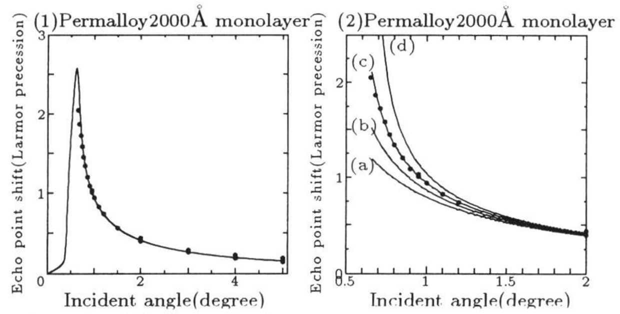

Fig. 6. The shift of NSE signals transmitted through magnetic permalloy45 thin film with thickness of 2000 Å as a function of incident angle. The closed circles were measured and the solid lines for (1) and calculated from matrix analysis of neutron spin rotation and of one-dimensional square potential for Schrödinger equation, and for (2) was calculated from the Larmor frequency ω_L and classical paths of neutron.

96.5neV, respectively.

As shown in Figs. 5 (1) and 6 (1), the closed circles measured values were well reproduced by the simulated line which is derived from the shift of NSE signal calculated by Eqs. (1.26) ~ (1.28) and matrix analysis of the neutron spin rotation. The lines include the effect of the distribution of wavelengths 5.08 ~ 6.52 Å. The peaks of both lines indicate the wavelength resolution and almost correspond to the closed circles measured, so that we confirm that the wavelength resolution for numerical simulation was adjusted to the experiments. As shown in Figs. 5(1), (2) and 6(1), (2), the Larmor precession is well interpreted as the traversal time through path (c) which is due only to the nuclear potential. The lines are the shift of NSE signal calculated from the classical Larmor frequency ω_L and four paths (a) ~ (d) as shown in Fig. 4 . The shift is given by

$$\gamma Bl / v_n - \gamma Hl / v_n \approx \gamma Bl / v_n \tag{3.1}$$

$$= \omega_L (l / v_n) = \omega_L t \tag{3.2}$$

$B \approx 1.6\times10^4 \gg 10^2 > H$ (Oe)

where B is the magnetic induction in the magnetic film, H the applied field at the sample position (guide field), v_n the neutron velocity and l is one of the paths of (a) ~ (d) as shown in Fig. 4 in the magnetic film.

Here the ratio of neutron velocity in a vacuum (air) and the sample is of order 10^{-5}, so we can consider the shift of NSE signal (echo point) as a function of the path length l. For iron with thickness of 790 Å and permalloy45 film with thickness of 2000 Å, the traversal time τ was estimated to be 2.1×10^{-8} sec at the incident angle of 0.58° and 4.4×10^{-8} sec at the incident angle of 0.65°, respectively.

We clearly confirmed the following points in the case of incident angles above the critical angle for total reflection:

1. The observed shifts of the NSE signals conform well to classical Larmor precession passing through a refracted path due only to the nuclear potential in a magnetic film.
2. The results of a numerical simulation based on Eqs. (1.26) ~ (1.28) and on a matrix analysis of neutron spin rotation reproduced well the observed shifts of the NSE signals. They correspond to the shift given by the product $\omega_L \tau$ of Larmor frequency ω_L and the traversal time τ.
3. Even in the vicinity of the critical angle, the extra classical Larmor precession is conserved.

1) For example, V. Nunez, C.F. Majkrzak and N.F. Berk, *Mat. Res. Soc. Symp. Proc.* 313 (1993) 431.
2) F. Mezei, ed., *Neutron Spin Echo, Lecture Notes in Physics* 128 (Springer, Heidelberg, 1980).
3) For example, W. Gavin Williams, *Polarized Neutron*, Clarendon Press Oxford, 1988.
4) F. Mezei, *Physica* B 151 (1988) 74.
5) For example, V.F. Sears, *Neutron Optics*, Oxford University Press, New York, Oxford 1989.
6) M. Büttiker, *Phys. Rev.* B 27 (1983) 6178.
7) M. Hino, N. Achiwa, S. Tasaki, T. Ebisawa and T. Akiyoshi, *Physica* B 213&214 (1995) 842.
8) N. Achiwa, M. Hino, S. Tasaki, T. Ebisawa and T. Akiyoshi, JAERI-M93-228 (JAERI CONF2) (1993) 738.
9) T. Ebisawa, S. Tasaki, T. Akiyoshi, N. Achiwa, S. Okamoto, *Annu. Rep. Res. Reactor Inst. Kyoto Univ.* 23 (1990) 46.
10) T. Kawai, T. Ebisawa, S. Tasaki, T. Akiyoshi, Y. Eguchi, M. Hino and N. Achiwa, KURRI-TR-406 (1995) 43.
11) T. Ebisawa, S. Tasaki, Y. Otake, H. Funahashi, K. Soyama, N. Torikai and Y. Matsushita, *Physica* B 213&214 (1995) 901.